MEASUREMENT OF DYNAMIC PERFORMANCE OF LARGE TILTING PAD JOURNAL BEARING AND ROTOR STABILITY IMPROVEMENT

by

Kyoichi Ikeno
Senior Mechanical Engineer

Yuichi Sasaki
Design Engineer
Mitsubishi Heavy Industries Compressor Corporation
Hiroshima, Japan

Ryou Kawabata
Research Engineer
Mitsubishi Heavy Industries, Ltd.
Hiroshima, Japan

Satoru Yoshida
Design Engineer
and
Satoshi Hata
Group Manager, Research and Development
Mitsubishi Heavy Industries Compressor Corporation
Hiroshima, Japan

Kyoichi Ikeno is the Senior Mechanical Engineer of the Turbine Design Section in the Engineering and Design Division, Mitsubishi Heavy Industries Compressor Corporation, in Hiroshima, Japan. He is a blade design specialist and has 12 years of experience with R&D for synthesis gas compressor steam turbines and gas turbines.

Mr. Ikeno has a B.S. degree from Miyazaki University and an M.S. degree (Mechanical Engineering) from Kyushu University.

Yuichi Sasaki is a Design Engineer in the Turbine Designing Section in the Engineering and Design Division, Mitsubishi Heavy Industries Compressor Corporation, in Hiroshima, Japan. He has three years of experience in designing steam turbines.

Mr. Sasaki has B.S. and M.S. degrees (Mechanical Engineering) from Kumamoto University.

Ryou Kawabata is a Research Engineer with the Structure & Vibration Laboratory in Mitsubishi Heavy Industries, Ltd., in Hiroshima, Japan. He has 10 years of experience in material strength evaluation.

Mr. Kawabata has an Associate's degree (Mechanical Engineering) from Kure National College of Technology.

Satoru Yoshida is a Design Engineer with the Compressor Designing Section in the Engineering and Design Division, Mitsubishi Heavy Industries Compressor Corporation, in Hiroshima, Japan. He has five years of experience in designing compressors.

Mr. Yoshida has B.S. and M.S. degrees (Mechanical Engineering) from Kobe University.

Satoshi Hata is a Group Manager within the Research and Development Group, Engineering and Design Division, at Mitsubishi Heavy Industries Compressor Corporation, in Hiroshima, Japan. He has 27 years of experience in R&D for nuclear uranium centrifuges, turbomolecular pumps, and heavy-duty gas turbines and steam turbines.

Mr. Hata has B.S., M.S., and Ph.D. degrees (Mechanical Engineering) from Kyusyu Institute of Technology.

ABSTRACT

Capacities at today's modern ethylene and refinery plants have steadily increased, giving rise to a growing demand for larger compressors and more powerful drivers all of which require larger rotating parts. In keeping with this trend, it is critically important to optimize the design of rotors, impellers and journal bearings for improved rotor dynamics and high performance fluid dynamics. Rotor stability itself can be greatly influenced by maintaining shorter bearing spans through careful impeller design and the proper selection of journal bearings, such as load-on-pad (LOP) or load-between-pad (LBP) types, and determining the correct number of pads.

In order to achieve a robust compressor design, case studies can be important tools in understanding the actual behavior and dynamic characteristics of large journal bearings. In this paper, the authors will present the results of a unique test to measure and compare the oil film profile, pressure and temperature along the bearing pad surface as well as the pad movement vibration for several types of journal bearings under rotating conditions. The dynamic data are compared with 3D finite element analysis/computational fluid dynamics (FEA/CFD) results for each type of journal bearing including rotor response comparison with experiment and analysis. The design and performance of improved impellers to create higher shaft rigidity and shorter bearing spans are also discussed. Finally, the authors will present their findings on optimum designs for large journal bearings and make recommendations on how to model journal bearings by separating each pad in the vibration system.

INTRODUCTION

During this decade, the capacity of ethylene plants has increased continuously as shown in Figure 1. Similarly, the flows of the high and low-pressure stages of the steam turbine have also increased. To meet this capacity increase, it is necessary to apply larger components including a larger inlet flow governing valve, long blades and larger rotors with longer bearing spans. The same is true on the compression side, where it is necessary to apply large impellers with long bearing span rotors. Compressors and turbine trains with capacities over 1.5 mtpy are already designed, manufactured and successfully operating at sites shown in the photograph of Figure 1. The same trend can be observed in LNG plants reaching to 9 mtpy.

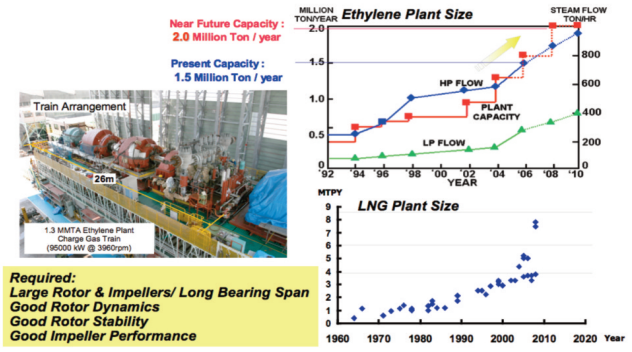

Figure 1. Ethylene and LNG Plant Size—Past and Future Trends.

In this situation, the basic requirements of good rotor dynamics, high rotor stability and excellent impeller performance are highlighted under the design conditions of large rotors/impellers with long bearing spans. In conjunction with robust designs that improve rotor dynamics and achieve higher fluid dynamic performance, the systematic optimization of rotors, impellers and journal bearings becomes very important.

Key elements in determining rotor stability include the selection of large size journal bearing types such as LOP or LBP with pad numbers 4 or 5. Also, impeller selections with high shaft rigidity and shorter bearing spans significantly impact total performance of large rotating equipment. To achieve a robust design of a large compressor, it is important to understand the actual behavior and dynamic characteristics of large journal bearings.

It is also important to deeply consider the basic direction for the compressor rotor optimization and its effect on stability of the unbalance response curve and critical map. As a first step, the authors introduce a survey of case study results comparing the key factors of the basic impeller shapes and their effect on impeller performance by CFD analysis, in order to apply compact short span impellers to actual machines. In addition, the static and dynamic strength analysis results are explained based on a detailed vibration analysis and impeller excitation stress measurement test.

It is explained how to determine the detail dimensions of an improved impeller to realize excellent performance comparing the existing impellers.

The actual behavior and dynamic characteristics for several types of large journal bearings under rotating conditions and stability improvement must be understood. It is also important to know the advantages and disadvantages of selecting LOP or LBP bearings with pad numbers 4 or 5 when considering the rotor rigidity and the actual bearing characteristics.

In this paper, the authors try to explain how to optimize the rotor dynamic vibration system based on the results of the bearing dynamic performance test and case study for rotor stability including bearing pedestal characteristics.

COMPRESSOR ROTOR OPTIMIZATION FOR RESPONSIBILITY AND STABILITY

The critical map for a specified rotor is very useful in understanding the rotor unbalance response and critical separation margin as shown in Figure 2. From the viewpoint of rotor stability, the authors have focused on the amplification factor and damping factor of the rotor parallel lowest frequency mode.

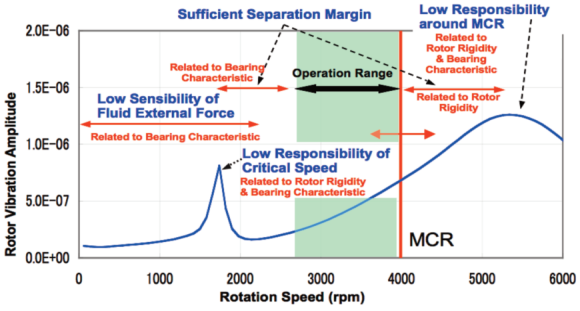

Figure 2. Compressor Rotor Optimization for Responsibility and Stability.

The key factors include low sensitivity to fluid external forces, low responsiveness to the first critical speed, low responsiveness around MCR (related to the first bending mode critical speed) and sufficient separation margins.

These key factors are affected by the individual bearing characteristics and rotor rigidity in varying degrees.

Focusing on the rotor characteristics, the first and second rotor bending mode is as shown in Figure 3. The ratio of 1st bending mode frequency at free-free support divided by MCR should be increased for the first mode higher stability and low sensitivity of

fluid external force. And the ratio of second bending mode frequency at free-free support divided by MCR should be increased for low responsiveness around MCR.

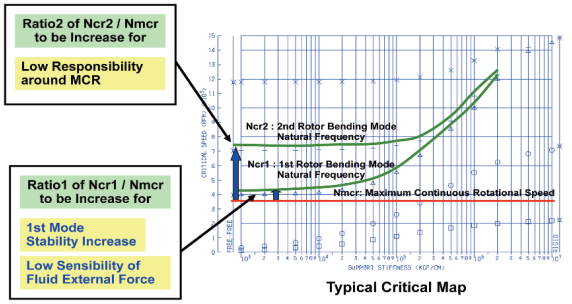

Figure 3. Compressor Rotor Rigidity Optimization for Stability Improvement on Critical Map.

In order to increase rotor rigidity, a balance between increasing the rotor shaft diameter and decreasing the bearing span must be considered and optimized. Figure 4 is a typical rotor rigidity map showing the basic index D/L^2 versus MCR for various rotor designs as well as the average proportional line based on experience of large compressor rotors. These rotors, designed using existing impellers, have the sufficient minimum logarithmic (log) decrement at the anticipated cross coupling according to API 617/684 Level II, and therefore, do not require a reduction in bearing span.

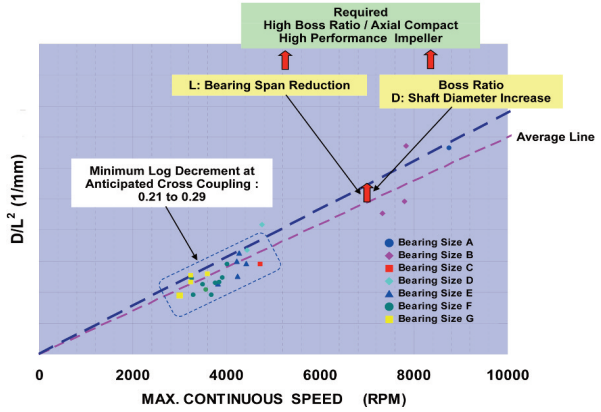

Figure 4. Large Compressor Rotor Rigidity Increase.

However, when the rotor design requires an increase in the number of impeller stages, the basic impeller dimensions must be changed including a reduction in axial length and an increase in the boss ratio as shown in Figure 5. Despite the negative impact on performance caused by these geometrical changes, it is necessary to maintain the performance of the improved impeller the same as required for the existing impeller.

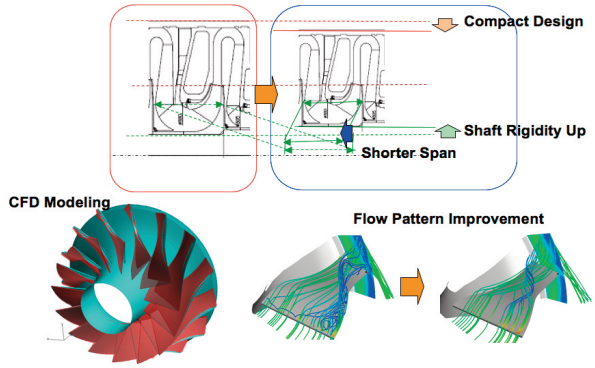

Figure 5. Compressor Impeller Optimization for Stability and Performance.

COMPRESSOR IMPELLER OPTIMIZATION FOR STABILITY AND PERFORMANCE

Referring to Figure 4, optimization of the new, compact impeller geometry requires balancing the impeller span reduction ratio and the boss ratio to achieve the required rotor rigidity and subsequently, overall rotor stability. The existing impellers are selected as a starting point for the case study to establish a reference for the impeller performance. Next, the new impeller profile is designed by CFD analysis. During the CFD analysis, the impeller span reduction ratio and boss ratio are varied and the impeller performance is calculated. The impeller stability and efficiency at the design point are chosen as the basic factors to evaluate the impeller performance. The calculation results are shown in Figure 6.

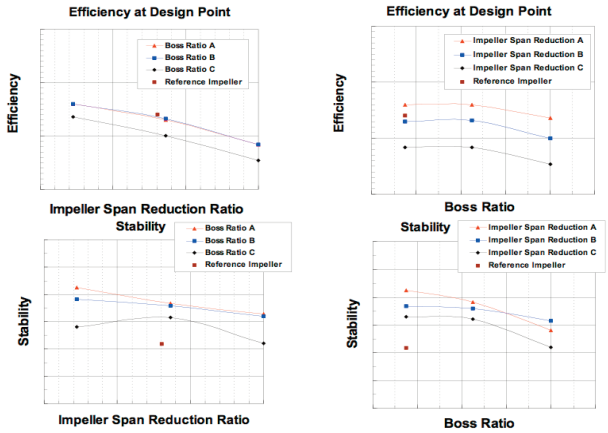

Figure 6. Compressor Impeller Optimization for Performance.

According to the analysis results for this prototype impeller, it is found that the efficiency is affected primarily by changes in the impeller span reduction ratio while the efficiency does not change over a certain range of the boss ratio. Beyond this certain range, the efficiency decreases. On the contrary, changes in the stability of the prototype impeller due to variations in the impeller span reduction ratio are not large and the stability does not change over a certain range of boss ratios but goes down beyond this range.

Finally the combination of impeller span reduction ratio and boss ratio are optimized to achieve maximum performance and rotor rigidity and to minimize the impeller mass and moment of inertia by application of the developed optimum design system. The results, the detail impeller profile and dimensions are finalized.

IMPELLER PERFORMANCE CFD ANALYSIS

In order to evaluate the overall performance of the impeller, diffuser and return vane, a CFD analysis is carried out. Figure 7 shows the Mach number profile for the improved impeller and return vane. In this analysis, the results confirmed that the improved impeller can control the flow while improving pressure change at the maximum flow coefficient. Efficiency in the low flow condition is also improved.

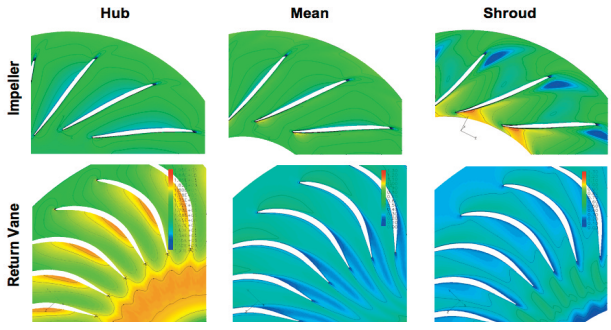

Figure 7. Mach Number Profile of Improved Impeller and Return Vane.

IMPELLER STRENGTH ANALYSIS

Figure 8 shows the results of the 3D FEA study conducted to evaluate the static stress and safety factor at the required maximum impeller rotating circumferential velocity. The average and local stress are lower than the criteria and a sufficient safety margin is confirmed.

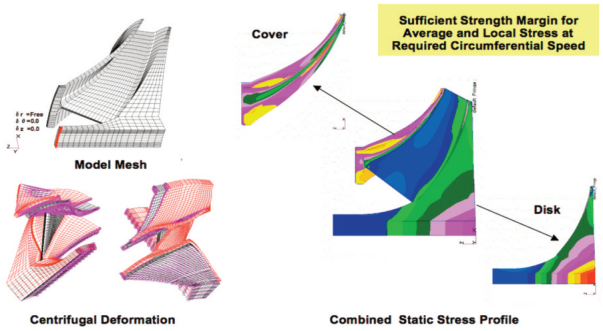

Figure 8. Improved Impeller Static Strength Evaluation.

And it is also important to evaluate the impeller vibration resonance, fluid dynamic excitation force and the resonance stress. During vibration analysis, the natural frequency of the coupled blade/shroud and disk mode is calculated and plotted on a nodal diameter interference diagram. Inlet guide vane wake excitation frequency zigzag line is added. According to the number of blades and inlet guide vanes, resonance nodal diameter number can be determined. The expected resonance point can be given at the cross point of this nodal diameter line and inlet guide vane wake excitation frequency zigzag line. From this nodal interference diagram, the first and second vibration modes at the 3 nodal-diameter are defined as shown in Figure 9. For each vibration mode and natural frequency, the modal mass, modal stiffness and the modal force are calculated. Accordingly, the relative stress profile per unit of the excitation force is also calculated from the system damping coefficient. To expect the actual dynamic stress profile of the impeller, the excitation force due to the inlet guide vane passing wake shall be calculated by CFD. The unsteady CFD analysis is conducted and the dynamic pressure change on impeller profile is calculated. The impeller vibration response due to the dynamic pressure change of fluid excitation on impeller blade profile is analyzed.

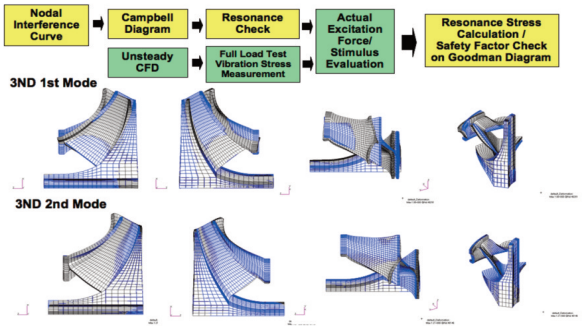

Figure 9. Impeller Vibration Analysis.

Referring to Higashio, et al. (2010), the authors introduce a unique technique for measuring stress on rotating blades during a full load test by specially designing flexible high response impellers to emphasize the vibration stress. The basic vibration characteristics of the nodal diameter interference diagram and Campbell diagram are explained. In order to estimate a vibration stress on the blades, an unsteady CFD analysis is applied for calculation of external excitation force and the vibration response is analyzed.

The detail results are systematically compared with the actual measured vibration stress and vibration response. Through this study, the resonance with inlet guide vanes (IGVs) and a unique blade/stator cascade interaction phenomena are found. The cause of these phenomena is investigated and the authors try to explain this mechanism. Finally, according to the correlation between the measured and analyzed vibration stresses by CFD over the whole flow path, the strength criteria are studied as a guideline by comparing application experience.

By correlation based on these test and analysis results, the actual vibration stress profile of this improved impeller is expected and sufficient strength safety margin of the improved impeller is confirmed.

IMPROVED IMPELLER PERFORMANCE TEST RESULTS

In order to evaluate the actual performance of the improved impeller as one stage, the test impeller is prepared by a two-piece manufacturing method. However, for the actual job impellers both one-piece and two-piece manufacturing methods can be applied depending on an impeller size. Figure 10 shows the performance test result of the improved impeller comparing to the exiting impeller. This improved impeller is designed to have the optimized combination features of impeller span reduction ratio and boss ratio to maximize performance and rotor rigidity while at the same time minimizing impeller mass and moment of inertia. The actual efficiency is higher than that of the original impeller in the same applicable flow coefficient range and it is confirmed that the surge margin and stability are the same as the original impeller design.

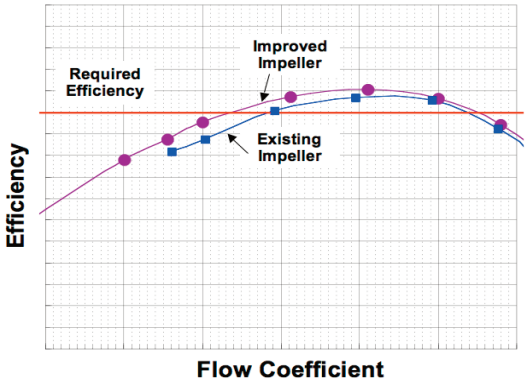

Figure 10. Improved Impeller Performance Measurement Results.

LARGE JOURNAL BEARING OPTIMIZATION FOR RESPONSIBILITY AND STABILITY

As explained above, the impeller design can be optimized to meet the required number of stages with improved performance and rotor rigidity. On the contrary, it is important to consider rotor response and rotor stability when selecting journal bearings suitable for large rotors. In previous technical symposia, a number of authors have provided excellent insight and useful suggestions in terms of journal bearing performance. Comparisons between LOP/LBP and pad number, measured and expected pad temperature and rotor stability are shown in Tables 1 and 2.

Table 1. Previous Excellent Works by Other Authors for Journal Bearings and Rotor Stability (A).

Gunter, 1972: **Rotor-Bearing Stability** **:Rotor Whirl Motion Characteristics, Stability Threshold vs Bearing Stiffness, Unbalance Response**
Nicholas and Kirk, 1979: **Selection and Design of Tilting Pad and Fixed Lobe Journal Bearings for Optimum Turborotor Dynamics (4LBP, 5LOP)** **:Stability Map and Growth Factor, K/C vs Preload, Rotor Response, Case Study for 2/8 Stage Rotor**
Salamone, 1984: **Journal Bearing Design Types and Their Application to Turbomachinery** **:Critical Map for Several Types of Journal Bearings**
Nicholas, et al., 1986: **Improving Critical Speed Calculations Using Flexible Bearing Support FRF Compliance Data** **:Support Shaker and Impact and Rotor Response**
Zeidan and Paquette, 1994: **Application of High Speed and High Performance Fluid Film Bearings in Rotating Machinery** **: 3/4/5/6 LOP/LBP K/C vs Orientation / Clearance, Support Flexibility and Rotor Response**

Table 2. Previous Excellent Works by Other Authors for Journal Bearings and Rotor Stability (B).

Nicholas, 1994:
Tilting Pad Bearing Design
: 5LBP/5LOP K/C vs Preload/Negative Preload, Sommerfeld Number
4LBP Pad Temperature vs Speed Measurement

DeCamillo and Brockwell, 2001:
A Study of Parameters that Affect Pivoted Shoe Journal Bearing Performance in High-Speed Turbomachinery
: 5LOP/5LBP Pad Temperature Profile Measurement

Nicholas and Kocur, 2005:
Rotordynamic Design of Centrifugal Compressors in Accordance with the New API Stability Specs.
:Stability Case Study for Several Industrial Application

He, et al., 2005:
Fundamentals of Fluid Film Journal Bearing Operation and Modeling (5LBP)
:Bearing Film Temperature Profile and Kxx/Kyy/Cxx/Cyy Characteristics Analysis and Measured Data

Kocur, et al., 2007:
Surveying Titling Pad Journal Bearing and Gas Labyrinth Seal Coefficients and Their Effect on Rotor Stability
:Non-synchronous / Synchronous Bearing /Seal Coefficient, Predicted Rotor Stability

DeCamillo, et al., 2008:
Journal Bearing Vibration and SSV Hash
: 5LOP-5LBP Mon-synchronous Low Frequency Vibration, Coefficient vs Oil Supply Flow

However, thus far there has not been any detailed study or discussion regarding the relationship between the types of bearings and the optimization of rotor stability and rotor response. The authors apply the unique measurement method to understand the bearing dynamic characteristics on line from the rotating rotor. In considering this difference from the previous studies by other authors, the large journal bearing technical evaluation and discussion points are explained in Table 3.

Table 3. Large Journal Bearing Technical Evaluation and Discussion Points.

Point-1:
Measurement of Dynamic Characteristics for Large Size Journal Bearing 4LBP/5LBP/5LOP in Detail and Calculation by CFD

Point-2:
Rotor Response for Large Size Journal Bearing 4LBP/5LBP/5LOP Comparison of Measured and Calculated Amplification Factor

Point-3:
Rotor Stability Depending on Journal Bearing Type 4LBP/5LBP/5LOP and Pedestal Dynamic Characteristics

Point-4:
What is the Optimized Design for Both of Low Unbalance-Response and Rotor Stability with Good Impeller Performance by Selecting Large Size Journal Bearing Type 4LBP/5LBP/5LOP and Rotor Rigidity by Reflecting Improved Short Span / High Boss Ratio Impeller

COMPARISON OF LOP/LBP TYPICAL TYPE JOURNAL BEARINGS

Table 4 shows the comparison of typical types of journal bearings, and for each bearing type, 4LBP, 5LBP and 5LOP, the key factors of static, dynamic and low speed friction loss are classified and listed in order to evaluate bearing performance. LBP type bearings can share the radial load by two pads and the pad temperature tends to be lower than LOP. The starting friction torque of LOP is relatively low compared to LBP because of wedge effect and high local intensity. In terms of dynamic characteristics such as the critical speed separation, vibration response and rotor stability, LBP and LOP types have advantages and disadvantages depending on the combination of bearing type and rotor rigidity.

Table 4. Comparison of Typical Type Journal Bearings Feature.

Load Type		Load Between Pad		Load On Pad
Pad Number		4 Pads	5 Pads	5 Pads
Pad Location Arrangement		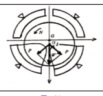	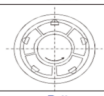	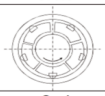
Static	Load Share	Better	Better	Good
	Friction Loss	Good	Good	Better
Dynamics	Critical Speed Separation	1H / 1V: Separation Margin Reduction	Characteristics between 4 LBP and 5 LOP	1H / 2H Large Separation Margin
	Vibration Response	1H / 1V: Separation Margin Reduction	Characteristics between 4 LBP and 5 LOP	1H / 2H Low Amplification Factor
	Stability	Sensitive for Fluid Excitation Depending on Rotor & Pedestal Rigidity	Sensitive for Fluid Excitation Depending on Rotor & Pedestal Rigidity	1H: Large Damping Log Decrement 2V: Depending on Rotor & Pedestal Rigidity
Low Speed Stating Torque		Better	Good	Good
Assembly / Clearance Control		Good	Good	Better
Oil Supply Flow		Good	Good	Good

The separation margin for first horizontal and vertical same critical speed (1H/1V) of the 4LBP type is less than the margin for first and second horizontal different critical speeds (1H/2H). 5LOP type bearings also have more damping effect and lower rotor response. LBP type bearings are sensitive to fluid excitation in the horizontal direction due to low damping effect and rotor stability depending on rotor rigidity and pedestal characteristics. 5LOP bearings have a large damping effect, log decrement for first horizontal critical mode response and second vertical critical mode depends on rotor rigidity and pedestal characteristics.

From the point of view of assembly and bearing clearance control, 5LOP is better than other types. Figure 11 is a typical critical map for several types of journal bearings and Figure 12 is a typical rotor response comparison for LOP and LBP bearings. It is easy to understand the difference between LBP and LOP, if comparing the line of bearing support stiffness and rotor natural frequency line for each mode in Figure 11, LOP can separate 1st/2nd Horizontal critical speed and first/second vertical critical speed widely. And 5LOP is very effective to use for bearing damping because of large relative vibrated displacement between the rotor and bearings.

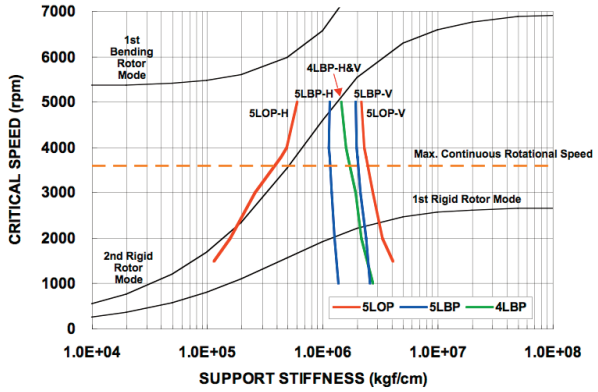

Figure 11. Critical Map for Several Types of Journal Bearings.

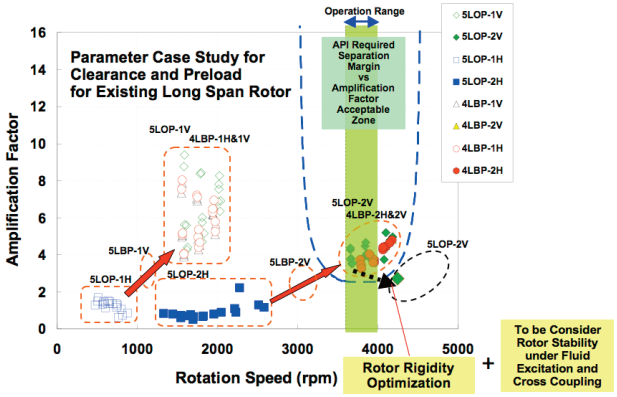

Figure 12. Rotor Response Comparison for LOP and LBP.

Figure 12 shows the parameter case study results of changing the bearing clearance and preload on a typical long bearing span/high stage number rotor in which the short span/high boss ratio improved impellers are not applied. Each zone of critical speed and amplification factor is classified for 4LBP, 5LBP, 5LOP in the horizontal and the vertical directions. At the same critical speed around 2000 rpm, comparing amplification factor of 5LOP-1H (horizontal) and 4LBP-1H reveals that the 5LOP damping is larger than 4LBP. And in comparing amplification factor of the 5LOP-1V and 4LBP-1V, 4LBP damping is relatively large but almost the same as 5LOP.

However, when considering the rotor stability for lowest critical mode excited by fluid cross term stiffness, the mode change between 2H of 5LOP and 1H of 4 LBP should be investigated as

Table of Contents

well as the sensitivity of rotor stability if cross term stiffness is increased in pursuit of a more robust rotor design.

Referring to Figure 12, this nonoptimized, long span rotor has a second critical speed within the operation range and therefore, cannot obtain the required separation margin. To achieve a sufficient separation margin, the rotor is redesigned to increase rigidity in the case of 5LOP bearing application. Finally 5LOP 2V critical speed can be increased.

On the contrary, it is necessary to thoroughly investigate the sensitivity for rotor stability due to cross term stiffness increase in view of what type of bearing, type (4LBP, 5LBP or 5LOP) shall be applied. As explained below, in terms of rotor stability sensitivity due to an increase in cross term stiffness, it is concluded that 5LOP is better than 4LOP. Finally, 5LOP and 5LBP are selected for the actual performance test.

TEST PROCEDURE FOR EVALUATION OF LARGE JOURNAL BEARING OF LOP/LBP

In order to verify the expected results of rotor response and stability, it is necessary to evaluate the actual large bearing characteristics for 5LOP and 5LBP by comparing the calculated bearing characteristics and the measured data especially under dynamic conditions. Dynamic bearing characteristics can be evaluated using the bearing shaker sweep excitation test in a rotating condition. In this paper, the authors try to evaluate the bearing performance by comparing the measured versus calculated unbalance response and unbalance effect vector based on the bearing coefficients calculated via 3D CFD analysis. The authors apply this unique measurement method in order to better understand the dynamic bearing characteristics on line from the rotating rotor in the test conditions shown in Table 5. The bearing size is 320 mm and 400 mm diameter. Unbalance response test, misalignment test and low speed turning test are conducted for 5LOP and 5LBP.

Table 5. Large Journal Bearing Technical Evaluation Conditions.

Case	Bearing Type	Rotation Speed (rpm)	Supply Oil Temperature (deg.C)	Oil Flow (L/min)	Misalignment (deg)	Test Condition
1	5LOP	1000,2000, 3000,3600, 3800	48	170 (φ320 mm) 200 (φ400 mm)	0	No Unbalance
2						With Unbalance
3		0 to 3800	48		0.06	Misalignment Test
5					0.1	
6		Low Speed controlled by Inverter	40,48,52		0	Turning Test 30min~8Hr
7	5LBP	1000,2000, 3000,3600, 3800	48		0	No Unbalance
8						With Unbalance
9		Low Speed controlled by Inverter	40,48,52		0	Turning Test 30min~4Hr

TEST SET UP

Figure 13 is the outline of the journal bearing test installation and Figure 14 is the test setup for the large journal bearings. The test rotor consists of a shaft and several disks that are assembled by shrink fit to adjust the rotor weight, bearing intensity and rotor rigidity. The support pedestals are designed to have sufficient stiffness and high natural frequencies beyond the operating speed range. The static deformation and each mode natural frequencies are calculated by 3D FEA as shown in the bottom of Figure 13. The pressure probe and clearance displacement probe are installed on the rotating rotor and the dynamic pressure continuous distribution and the oil film thickness continuous distribution can be measured for the bearings on both sides. The rotor vibration is measured from the pedestal (relative vibration) and the base plate (absolute level on the earth).

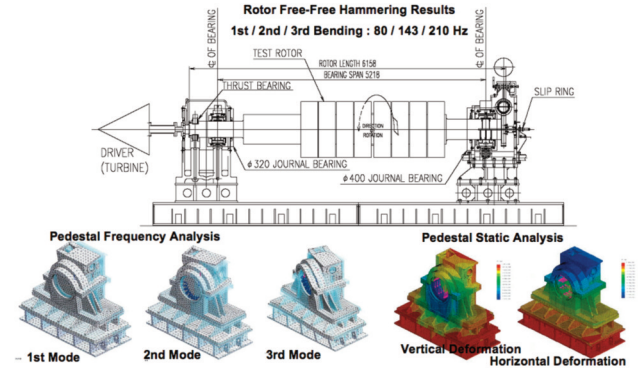

Figure 13. Outline of Journal Bearing Test Installation.

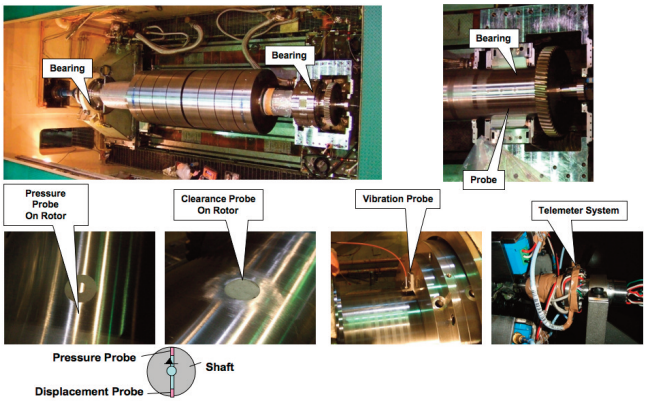

Figure 14. Test Setup for Large Journal Bearings.

Figure 15 is the large size journal bearing and pad temperature measurement locations. The temperature probes are installed on each pad at the oil inlet, hot point and oil exit.

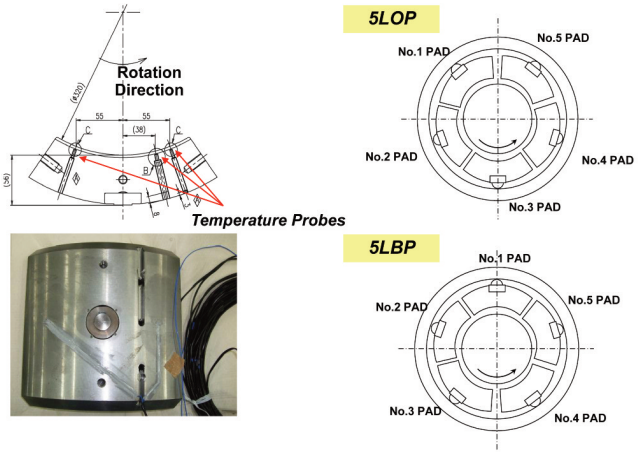

Figure 15. Large Size Journal Bearing and Pad Temperature Measurement Location.

TEST RESULTS OF LARGE JOURNAL BEARING PERFORMANCE

Figure 16 is the typical oil film temperature profile of 5LOP versus 5LBP bearings comparing the calculated temperature and other measurement results. The measured oil film temperature profile for each case is in good agreement with the theoretical calculation and in case of 5LBP, the maximum oil film temperature is lower than that of 5LOP due to the pressure intensity difference and load sharing over two pads. As shown in Figure 17, the calculated relation of oil film temperature versus speed is almost coincident with the measurement for both cases of 5LOP/5LBP.

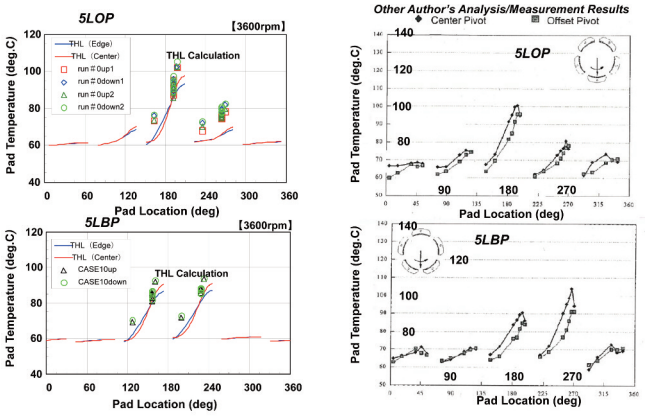

Figure 16. Typical Oil Film Temperature Profile of 5LOP Versus 5LBP.

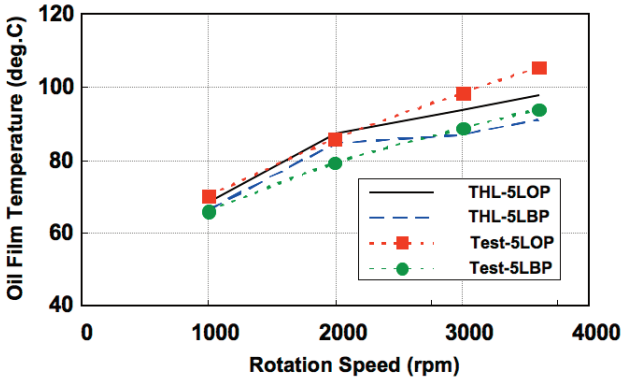

Figure 17. Typical Oil Film Temperature Versus Speed of 5LOP/5LBP.

In Figure 18, the typical oil film pressure profile of 5LOP and 5LBP are compared. The calculated maximum oil pressure and its location on the pad are almost the same as the measurement.

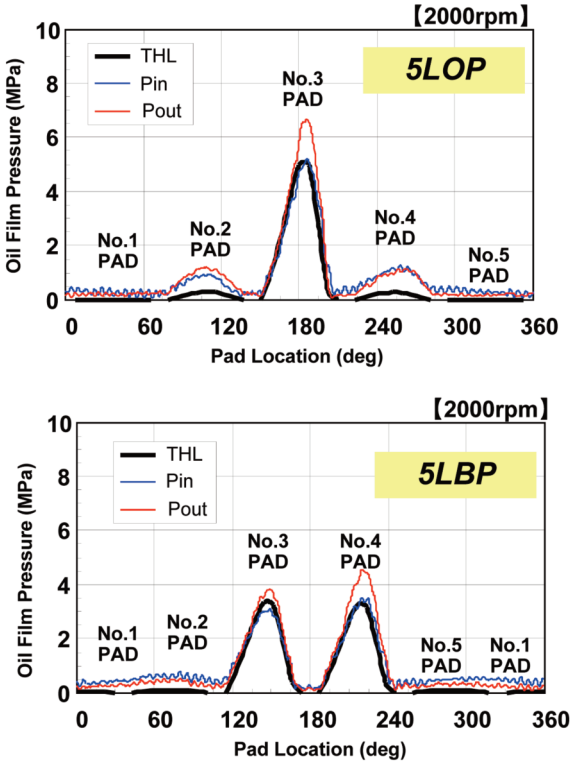

Figure 18. Typical Oil Film Pressure Profile 5LOP Versus 5LBP.

In Figure 19, the typical oil film thickness profile for 5LOP and 5LBP is shown. The physical relationship of oil film temperature, oil film pressure and oil film thickness are coincident with the calculation and measurement. The calculated oil film is larger than the measurement for both cases, 5LOP and 5LBP. The difference between the calculation and measurement for high pad loading is smaller than light pad loading such as side pads in the horizontal direction. In both cases, 5LOP and 5LBP, the pads in the horizontal direction share more load. In this sense, it is expected that the actual stiffness and damping in the horizontal direction are larger than the calculated characteristics and affect the rotor response and stability.

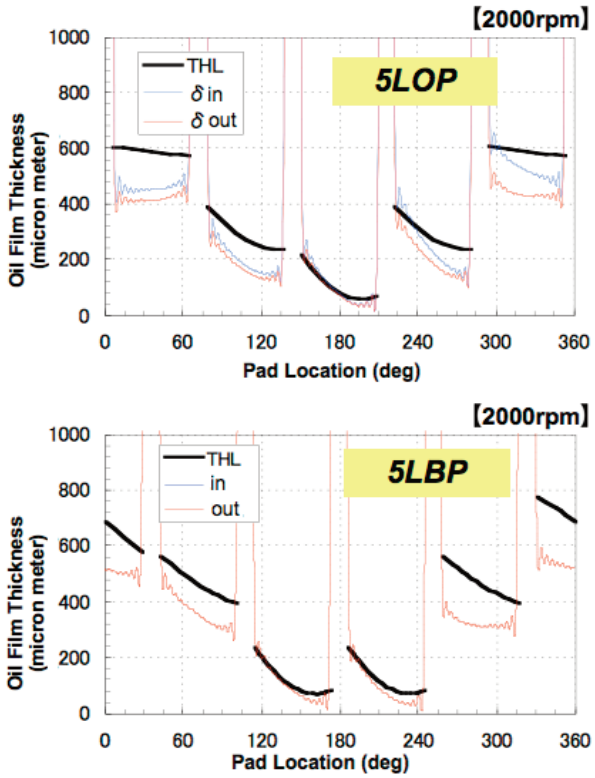

Figure 19. Typical Oil Film Thickness Profile 5LOP Versus 5LBP.

The spragging and pad flutter terms are used to describe the damage often found on the leading edge of unloaded pads in large steam turbine, compressor and generator units. In some cases, momentary contact with the pivot occurs once per cycle. In general, the smaller the arc angle, the more stable the pad motion. The authors try to investigate this flutter phenomenon for large journal bearings located on the top half unloaded condition.

Figure 20 is the measured result of pad partial vibration phenomena and Figure 21 is the fast Fourier transform (FFT) analysis results during speed change. In comparing the pad vibration wave phase of the axial direction motion (delta-2 and delta-3) and circumferential direction (delta-1 and delta-2) in Figure 20, a phase difference in the rotating circumferential direction at 2000 rpm is observed. This phenomenon is caused by the unloaded pad flutter. In case of increasing speed and oil film pressure, this flutter phenomenon disappears. According to FFT analysis results, in the speed range of 1600 rpm to 2800 rpm, the flutter vibration amplitude is about 540 micron meter and the expected maximum oil film pressure is 0.54 kgf/cm^2. The flutter frequency is 3 to 4 Hz at 350 rpm and 17 to 27 Hz at 1600 rpm to 2800 rpm. On the contrary, the pad natural frequency in the condition of no pressure support on oil film and free-free support is expected to be 2700 Hz, which is higher than this flutter low frequency. These findings show that flutter is not caused by pad resonance phenomenon.

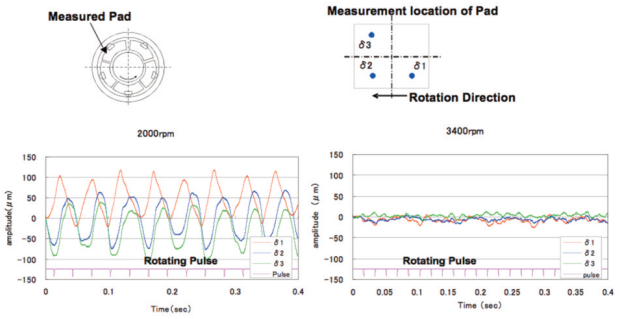

Figure 20. Pad Partial Vibration Phenomena (A).

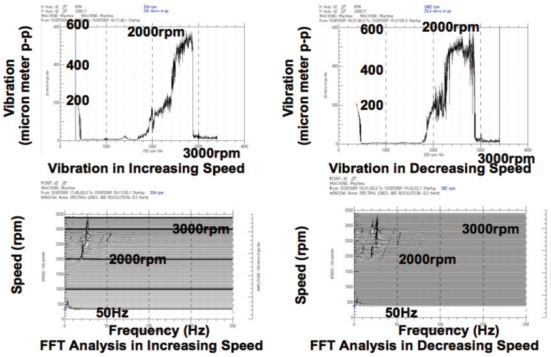

Figure 21. Pad Partial Vibration Phenomena (B).

ROTOR DYNAMIC RESPONSE TEST AND CALCULATION FOR LOP/LBP

As stated earlier, evaluation of dynamic bearing characteristics can be made using the bearing shaker sweep excitation test in a rotating condition. Considering the whole vibration system—including rotor and pedestal—the authors try to evaluate the bearing performance by comparing the measured versus calculated unbalance response and unbalance effect vector based on the bearing coefficients calculated via 3D CFD analysis. In order to verify the rotor modeling, the rotor hammering test is conducted and the results are compared with analysis results for the first to the third bending mode.

Table 6 shows the rotor dynamic analysis and measured response comparison. In both cases, 5LBP and 5LOP, the measured first critical speed in the horizontal and vertical directions is coincident with the calculation. The amplification factor in the horizontal direction for 5LBP is larger than that of 5LOP and the measured amplification factor is almost the same as calculated. However a large difference between the measured and calculated values is observed in the vertical direction. It should be noted that the test rotor is designed to have a sufficiently high amplification factor for evaluation.

Table 6. Rotor Dynamic Analysis and Measured Response Comparison.

Bearing Type	Analysis Condition			Horizontal		Vertical	
	Case	Pedestal Condition Cω/K	Bearing Damping Condition	Critical Speed (rpm)	Amplification Factor	Critical Speed (rpm)	Amplification Factor
5LBP	Measured	-	-	1244	14.8	1389	29
	1	0.1	Calculated	1236	11.0	1398	16.7
	2	0.05	Calculated	1235	13.6	1397	20.7
	3	0.025	Calculated	1235	15.5	1397	23.6
5LOP	Measured	-	-	No Critical		1387	33.6
	1	0.1	Calculated	719	1.7	1416	19
	2	0.05	Calculated	721	1.7	1415	24.9
	3	0.025	Calculated	722	1.7	1415	29.4

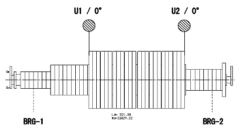

The amplification factor is affected by the pedestal stiffness and structure damping. In the case study, additional calculations are conducted by changing the ratio of Cω/K (damping × frequency divided by stiffness) from 0.1, 0.05 and 0.025 as shown in Table 6. In order to evaluate the rotor response, it is necessary to measure the actual pedestal characteristics. The hammer test is carried out on the pedestals with and without the rotor installed. The results are shown in Figure 22, Tables 7 and 8, and Figure 23.

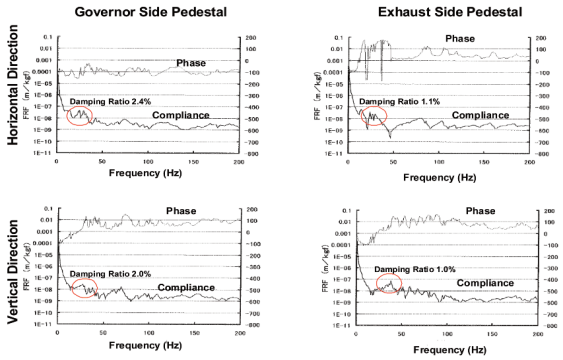

Figure 22. Typical Hammering Test Results of Large Rotor Pedestal.

Table 7. Vibration Response Results of Several Pedestals (A).

Pedstal Case	No.	Horizontal Direction					
		Natural Frequncy f (Hz)	Damping Ratio ζ(%)	Equivalent Rigidity K(kg/cm)	Modal Mass m(kgs²/cm)	Damping Coefficient Cω (kg/cm)	Pedestal Loss Coefficient Cω/K
Case-1	1	82	5.4	1.0E+06	3.9	1.1E+05	0.109
No Rotor	2	110	3.5	1.9E+06	3.9	1.3E+05	0.071
Case-2	3	86	4.3	1.4E+06	4.9	1.3E+05	0.087
No Rotor	4	73	6.1	2.1E+06	10.0	2.5E+05	0.122
Case-3	5	80	5.8	7.8E+05	3.1	9.0E+04	0.116
No Rotor	6	75	5.5	1.5E+06	6.7	1.6E+05	0.109
Case-4	7	78	4.4	1.5E+06	6.4	1.3E+05	0.087
No Rotor	8	67	4.7	1.5E+06	8.5	1.4E+05	0.093
Case-5	9	81	4.4	2.0E+06	7.7	1.7E+05	0.087
No Rotor	10	66	4.7	1.4E+06	8.1	1.3E+05	0.093
Case-6	11	60	2.4	1.0E+06	7.0	4.8E+04	0.048
Rotor On	12	100	15.0	2.0E+06	5.1	6.0E+05	0.300

Modal Mass $m = K/(2\pi F)^2$

Damping Coefficient $C\omega = 2\zeta m(2\pi f)^2$

Table 8. Vibration Response Results of Several Pedestals (B).

Pedstal Case	Vertical Direction					
	Natural Frequncy (Hz)	Damping Ratio ζ(%)	Equivalent Rigidity KP(kg/cm)	Modal Mass m(kgs²/cm)	Damping Coefficient CωP (kg/cm)	Pedestal Loss Coefficient Cω/K
Case-1	190	4.3	1.0E+07	7.3	8.9E+05	0.086
No Rotor	177	4.3	3.7E+06	3.0	3.2E+05	0.087
Case-2	166	9.3	3.8E+06	3.5	7.0E+05	0.186
No Rotor	129	5.3	5.7E+06	8.7	6.0E+05	0.106
Case-3	165	13.0	2.1E+06	2.0	5.6E+05	0.261
No Rotor	129	5.2	5.2E+06	8.0	5.5E+05	0.105
Case-4	123	2.0	1.7E+07	29.1	6.8E+05	0.040
No Rotor	127	4.0	5.4E+06	8.5	4.3E+05	0.080
Case-5	122	2.0	1.9E+07	32.0	7.4E+05	0.040
No Rotor	130	4.0	6.0E+06	9.0	4.8E+05	0.080
Case-6	60	1.1	1.0E+06	7.0	2.2E+04	0.022
Rotor On	100	15.0	2.0E+06	5.1	6.0E+05	0.300

Modal Mass $m = K/(2\pi F)^2$

Damping Coefficient $C\omega = 2\zeta m(2\pi f)^2$

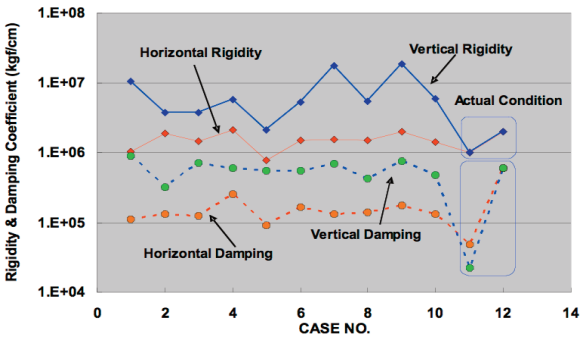

Figure 23. Vibration Response Results of Several Pedestals.

In Figure 22, compliance (the reverse of dynamic stiffness) for the horizontal and vertical directions is shown. According to the response curve, the damping ratio can be evaluated in the frequency range of operation by the typical hammer test for the large rotor pedestal.

In Tables 7 and 8, the natural frequency, damping ratio, equivalent rigidity and pedestal loss coefficient are summarized and for each case, the rigidity and damping coefficient are plotted in Figure 23. From these results, the pedestal loss coefficient with the rotor installed is expected to be the range of 0.02 to 0.3. In this large bearing performance test, the pedestal loss coefficient is expected to be in the same range and according to the case study of rotor response calculation, the amplification factor comes close to the measured data.

ROTOR UNBALANCE EFFECT VECTOR COMPARISON OF CALCULATION AND MEASUREMENT FOR LOP/LBP

As the authors discussed above, the measured unbalance rotor response and the amplification factor for this unbalance are evaluated as systematic characteristics of journal bearings. Also, the unbalance effect vector of rotor response is an important factor to evaluate the bearing characteristics. By subtracting the response values (with and without unbalance), the unbalance effect vector can be obtained. The vector's amplitude and phase with increased rotational speed are shown in Figure 24 for 5LOP in the vertical direction and Figure 25 for 5LOP in the horizontal direction, respectively, in comparing calculation results. In the vertical and horizontal directions, both the amplitude and phase coincide well with the calculation and in the horizontal direction, the rotor response can be overdamped well as compared to the case of 5LBP as explained below.

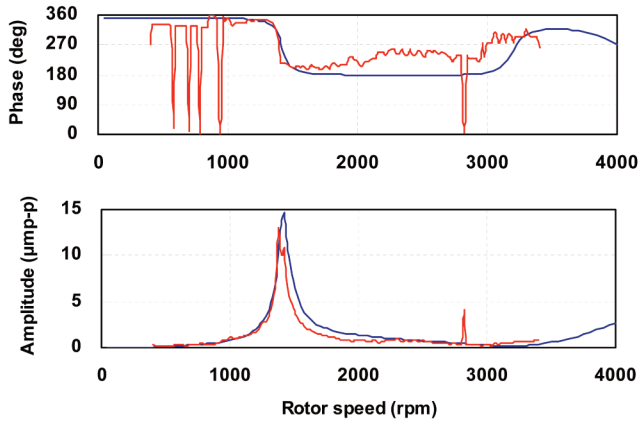

Figure 24. 5LOP Unbalance Response Effective Vector Phase and Amplitude for Vertical Direction.

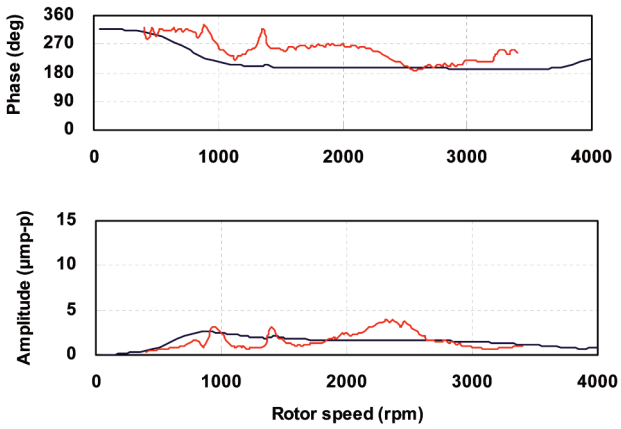

Figure 25. 5LOP Unbalance Response Effective Vector Phase and Amplitude for Horizontal Direction.

In case of 5LBP, the unbalance effect vector is obtained and the vector's amplitude and phase with increased rotational speed are shown in Figure 26 for 5LOP in vertical direction and Figure 27 in horizontal direction, respectively, in comparing calculation results. In the vertical direction, the amplitude and phase coincide well with the calculation. However, in the horizontal direction, the rotor response cannot be damped and the amplification factor is larger than in the case of 5LBP, as explained in Figure 12 and the calculated amplitude is larger than the measurement. This difference is shown in polar plot form in Figure 28. The modal circles for calculated and measured values are in good agreement in the vertical and horizontal directions but do not compare well in horizontal amplitude.

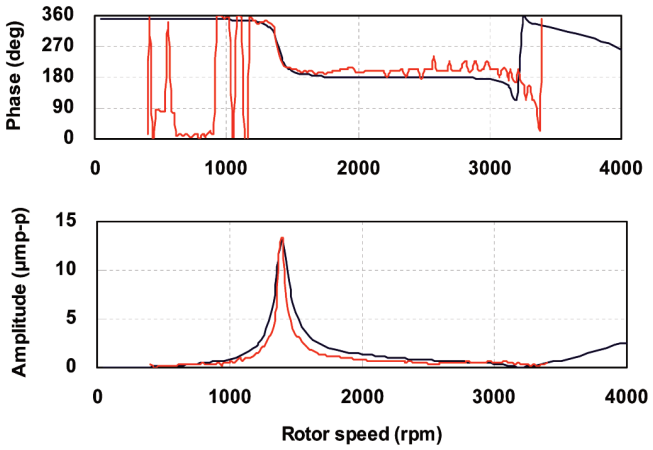

Figure 26. 5LBP Unbalance Response Effective Vector Phase and Amplitude for Vertical Direction.

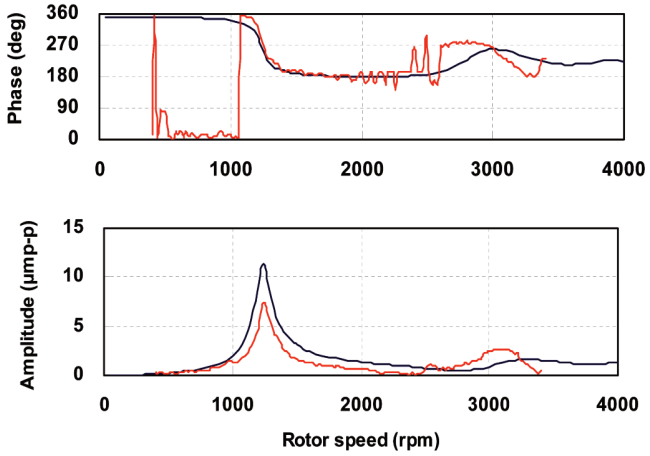

Figure 27. 5LBP Unbalance Response Effective Vector Phase and Amplitude for Horizontal Direction.

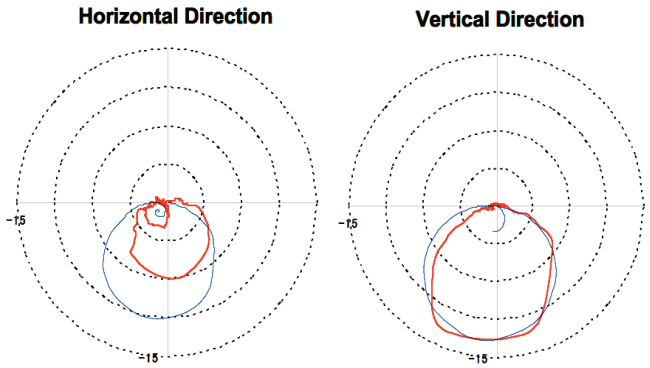

Figure 28. 5LBP Unbalance Response Effective Vector Polar Diagram for Horizontal and Vertical Direction.

The reason for the difference in calculated and measured amplitudes in the horizontal direction for the 5LBP has to be investigated by an additional study. From this study, it is concluded that the bearing characteristics and systematic rotor response can be precisely predicted using state-of-the-art CFD analysis. Also, from the viewpoint of systematic rotor vibration analysis, the evaluation of pedestal characteristics is very important.

COMPRESSOR STABILITY CASE STUDY FOR SEVERAL TYPES OF JOURNAL BEARINGS

According to the discussion results above, the authors have explained how to determine the detailed dimensions for an optimized impeller design that improves rotor rigidity and compressor performance. Furthermore, the actual behavior and dynamic characteristics for several types of large journal bearings, under rotating conditions, have been examined in an effort to improve overall stability. Similarly, the advantages and disadvantages in the selection of LOP or LBP bearing types and pad numbers 4 or 5 have been compared in terms of rotor rigidity and bearing characteristics. Finally, this paper attempts to explain how to optimize the rotor dynamic vibration system based on the results of the bearing dynamic performance test and the case study of rotor stability including pedestal characteristics using optimized impellers with short spans and high boss ratios.

The authors chose a planned mega ethylene plant for this case study as shown in Figure 29. If existing impellers are applied, the large propylene train would require two casings. On the contrary, by optimizing the impeller designs with a compact span and high boss ratio, one casing compressor can be selected. Based on the optimization of the fluid dynamic performance, rotor rigidity and critical separation margins, the authors have carried out the case study for rotor stability with different bearing types and pedestal characteristic according to API 617/684 Level II. The analysis results are shown in Figure 30. From the interesting evaluation results, the following points are found.

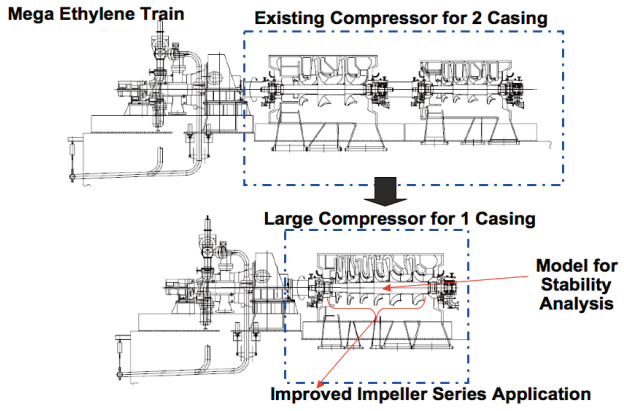

Figure 29. Compressor Rotor Stability Typical Model of Case Study.

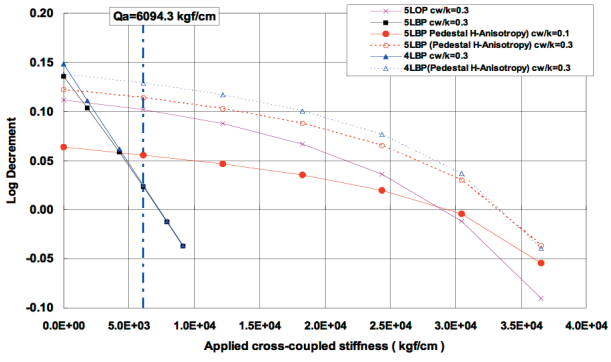

Figure 30. Compressor Stability Case Study for Several Types of Journal Bearings.

When no cross-coupled stiffness caused by dynamic and transient fluid excitation unstable force is applied, the log decrement due to bearing damping effect for 4LBP and 5LBP is larger than that of 5LOP. However, when the cross-coupled stiffness is applied, the log decrement decreases remarkably. On the contrary, in case of 5LOP, the log decrement does not decrease very much even if the applied cross-coupled stiffness increases.

When considering the reason for this remarkable stability difference between LBP and LOP, the anisotropy of bearing stiffness and vibration orbit in the horizontal and vertical direction should be considered. In addition, the bearing vibration of LBP is the pure forward vibration as shown in Figure 28. On the contrary, the bearing vibration of LOP is the linear summation of forward and backward vibration. Consequently, the oval orbit in the horizontal direction occurs.

This oval orbit changes due to the liner summation of each stiffness Kxx and Kxy or Kyy and Kyx. Furthermore, Kxy and Kyx causes a pure circle, same as the LBP orbit. The rotor vibration mode changes due to the difference of bearing stiffness in the case of increasing the applied cross-coupled stiffness Kxy, Kyx.

The key factor determining that the rotor is stable is the energy plus/minus balance, which is directly related to balance of forward and backward vibration. Under this condition, the cross term stiffness that affects on only forward direction can make the vibration system unstable. The backward direction (minus) has the effect of becoming stable (plus).

Another finding from this case study is that if the damping or stiffness in the horizontal direction is anisotropic and can be controlled to increase the pedestal loss coefficient in case of LBP, the pure circle orbit can be changed to the oval orbit the same as the LOP bearing, and the stability can be increased. However, in practical thinking, it is not easy to control the stiffness and damping in both directions.

According to the above investigation, it is concluded to apply 5LOP for the large, long span compressor rotor supported by large journal bearings.

CONCLUSIONS

Based on the present trend toward larger petrochemical plant sizing, the demand for higher power requirements and larger rotor sizing of the main rotating equipment will continue. In order to achieve a robust rotor design with improved rotor dynamics and fluid dynamics, the systematic optimization of the rotor, impellers and journal bearings becomes very important.

In this paper, the authors carried out a unique test for several types of large journal bearings by using an equivalent large rotor to measure the profile of the oil film, the pressure and temperature along each pad surface and the pad movement vibration under rotating conditions. The dynamic data are compared with the results of 3D FEA/CFD for each type of journal bearing including a rotor response comparison with experiment and analysis.

The performance results of the improved impeller designs that optimize shaft rigidity and reduce the bearing span are also introduced. In choosing a typical improved large compressor impeller and rotor, the stability analysis is conducted as a case study for LOP or LBP bearings with pad numbers 4 and 5.

Finally, the authors have explained what the optimum design for large size journal bearings is and it is concluded to apply 5LOP journal bearings for the large, long span compressor rotor for the large train configuration of a mega ethylene plant and LNG.

REFERENCES

DeCamillo, S. M. and Brockwell, K., 2001, "A Study of Parameters that Affect Pivoted Shoe Journal Bearing Performance in High-Speed Turbomachinery," *Proceedings of the Thirtieth Turbomachinery Symposium*, Turbomachinery Laboratory, Texas A&M University, College Station, Texas, pp. 9-22.

DeCamillo, S. M., He, M., and Cloud, C. H., 2008, "Journal Bearing Vibration and SSV Hash," *Proceedings of the Thirty-Seventh Turbomachinery Symposium*, Turbomachinery Laboratory, Texas A&M University, College Station, Texas, pp. 11-23.

Gunter, E. J., Jr., 1972, "Rotor-Bearing Stability," *Proceedings of the First Turbomachinery Symposium*, Turbomachinery Laboratory, Texas A&M University, College Station, Texas, pp. 119-141.

He, M., Cloud, C. H., and Byrne, J. M., 2005, "Fundamentals of Fluid Film Journal Bearing Operation and Modeling," *Proceedings of the Thirty-Fourth Turbomachinery Symposium*, Turbomachinery Laboratory, Texas A&M University, College Station, Texas, pp. 155-175.

Higashio, A., Yamashita, H., and Ota, M. 2010, "Dynamic Stress Measurement of Centrifugal Compressor Impeller and Study for Strength Criteria Based on Correlation by Unsteady CFD," *Proceedings of the Thirty-Ninth Turbomachinery Symposium*, Turbomachinery Laboratory, Texas A&M University, College Station, Texas.

Kocur, J. A., Jr., Nicholas, J. C., and Lee, C. C., 2007, "Surveying Tilting Pad Journal Bearing and Gas Labyrinth Seal Coefficients and Their Effect on Rotor Stability," *Proceedings of the Thirty-Sixth Turbomachinery Symposium*, Turbomachinery Laboratory, Texas A&M University, College Station, Texas, pp. 1-10.

Nicholas, J. C., 1994, "Tilting Pad Bearing Design," *Proceedings of the Twenty-Third Turbomachinery Symposium*, Turbomachinery Laboratory, Texas A&M University, College Station, Texas, pp. 179-194.

Nicholas, J. C. and Kirk, R. G., 1979, "Selection and Design of Tilting Pad and Fixed Lobe Journal Bearing for Optimum Turborotor Dynamics," *Proceedings of the Eighth Turbomachinery Symposium*, Turbomachinery Laboratory, Texas A&M University, College Station, Texas, pp. 43-57.

Nicholas, J. C. and Kocur, J. A., 2005, "Rotordynamic Design of Centrifugal Compressors in Accordance with the New API Stability Specifications," *Proceedings of the Thirty-Fourth Turbomachinery Symposium*, Turbomachinery Laboratory, Texas A&M University, College Station, Texas, pp. 25-34.

Nicholas, J. C., Whalen, J. K., and Franklin, S. D., 1986, "Improving Critical Speed Calculations Using Flexible Bearing Support FRF Compliance Data," *Proceedings of the Fifteenth Turbomachinery Symposium*, Turbomachinery Laboratory, Texas A&M University, College Station, Texas, pp. 69-78.

Salamone, D. J., 1984, "Journal Bearing Design Types and Their Applications to Turbomachinery," *Proceedings of the Thirteenth Turbomachinery Symposium*, Turbomachinery Laboratory, Texas A&M University, College Station, Texas, pp. 179-192.

Zeidan, F. Y. and Paquette, D. J., 1994, "Application of High Speed and High Performance Fluid Film Bearings in Rotating Machinery," *Proceedings of the Twenty-Third Turbomachinery Symposium*, Turbomachinery Laboratory, Texas A&M University, College Station, Texas, pp. 209-233.

ACKNOWLEDGEMENT

The authors gratefully wish to acknowledge the following individuals for their contribution and technical assistance in analyzing and reviewing the results and for their great suggestions and leading of practical application and testing: N. Nagai, A. Nakaniwa of Mitsubishi Heavy Industries, Ltd, and M. Sicker of Mitsubishi Corporation Houston.